Methodology of Extracting Sea Ice Motion Vectors from Geostationary Meteorological Satellite Data

MATSUMOTO Takanori [1] and IMAI Takahito [2]

Abstract

The Japan Meteorological Agency monitors sea ice in the Sea of Okhotsk every winter using a Geostationary Meteorological Satellite (GMS).

There are not many observations on wind, sea surface currents and tidal waves on a local space-time scale that can be used to estimate sea ice motion. Therefore, using satellite data is an effective way of measuring sea ice motion.

This paper mentions the scheme of Sea Ice Motion Vector calculations from GMS and the elimination of other motion vectors, treating them as noise. By the thresholds of two statistical values, almost all the effects from other motion vectors are eliminated.

This paper is a review of Matsumoto 2000 and 2003. The scheme used in the research has been used in the Meteorological Satellite Center since January 2007. A newly defined value $R_{i,j}$ is used to confirm the width of the template, and the aim of this paper is to explain the extraction of sea ice motion vectors.

1 Introduction

The Japan Meteorological Agency (JMA) issues sea ice information in the Sea of Okhotsk every winter from December to May. Sea ice analysis charts and sea ice forecasts are included in this sea ice information. Monitoring sea ice and forecasting its movements are very important for socio-economic activities, because in some cases, sea ice obstructs shipping or damages marine products and fishery facilities. Changes in the sea ice condition depend on the sea ice motion generated by wind and sea surface currents. Therefore, sea ice motion vectors are one of the necessary components of JMA's sea ice information. But there are not many observations of sea ice motion that have measured it qualitatively from ships and coastal stations.

On the contrary, there are many satellites that can observe sea ice from space. To measure sea ice, which is distributed on the sea in a wide area, satellite data are useful.

Usually, sea ice exists in polar regions which geostationary satellites cannot observe and only data from polar orbit satellites is available. Polar orbit satellites with microwave sensors are useful for sea ice observation because they can detect sea ice even through clouds. The spatial resolution of such microwave sensors is at most 12 km and the time interval between observations is about 12 hours.

Because the Sea of Okhotsk is the southernmost area in which sea ice appears widely, data of JMA GMS series at 140E longitude are also useful. The spatial resolution of the sensors on JMA GMS is shown in Table 1. The resolution of the infrared

[1] System Engineering Division, Data Processing Department, Meteorological Satellite Center

[2] System Engineering Division, Data Processing Department, Meteorological Satellite Center (Present affiliation: Forecast Division, Forecast Department, Japan Meteorological Agency)

(Recieved July 27, 2007, Accepted December 21, 2007)

channel data in GMS is coarser than that of the visible channel data. The resolution of visible channel data in GMS around the Sea of Okhotsk is about 1.5 km. Therefore, the visible images of GMS have the advantage that they allow observations to be made in short intervals of time and on a small scale.

Sea ice motion is observed by tracking a target ice floe or lead in an ice field. When tracking the target on a satellite image, the cross correlation method is the standard method for deriving sea ice motion (Emery et al., 1995). This is also used for atmospheric motion vector (AMV) product, which is derived from the motion of cloud and water vapor patterns on satellite images.

Since sea ice moves slower than clouds, a longer time interval is needed to calculate sea ice motion compared with calculating cloud motion. On the contrary, using images taken at longer time intervals means the effects of clouds increase. Therefore, in this paper, the time interval to calculate sea ice motion vector is set at two hours. To extract sea ice motion from GMS data, it is necessary to remove the data of motions that are not tracing sea ice. And, targets which have a subgrid scale displacement cannot be traced. Because of the characteristics of visible and infrared channels, sea ice under clouds cannot be observed. In the winter, convective cloud cells are generated all over the Sea of Okhotsk simultaneously. These cloud cells prevent us from recognizing sea ice from GMS data.

This paper mentions a method to get sea ice motion vectors from GMS visible images. Section 2 explains the maximal cross correlation method and the setting of the size of template and search areas. In section 3, two statistic values “entropy” and “value of uniformity in direction” are introduced as a quality check of derived vectors to remove those vectors that do not trace sea ice. Entropy is a measure of the uncertainty associated with random variables. In communication theory, entropy is defined as the degradation of a digital signal as it travels through a data telecommunication line (Shannon, 1948). But in image analysis, entropy is used to represent the randomness of the values of pixels in an image.

Table 1. Specifications of the sensors on geostationary meteorological satellites used in the Japan Meteorological Agency.

Satellite	MTSAT-1R		GOES-9		GMS-5		MTSAT-2	
Imager	JAMI		Imager		VISSR		Imager	
Operation (West Pacific)	28 Jun. 2005 to present		22 May 2004 to 28 Jun. 2005		13 Jun. 1995 to 22 May 2004		(2010 to 2015)	
Geo. Position	140E		155E		140E		145E	
Raw Data Format	HRIT		GVAR		VISSR		HRIT	
Number of channel	5		5		4		5	
Band	Wavelength (μm)	Accuracy	Wavelength (μm)	Accuracy	Wavelength (μm)	Accuracy	Wavelength (μm)	Accuracy
VIS(Visible)	0.55-0.90	6.5SNR@2.5%	0.55-0.75	(NA)	0.55-0.9	6.5SNR@2.5%	0.55-0.80	6.5SNR@300K
IR1(IR window 1)	10.3-11.3	0.18@300K	10.2-11.2	0.11@300K	10.5-0.9	0.35@300K	10.3-11.3	0.11@300K
IR2(IR window 2)	11.5-12.5	0.18@300K	11.5-12.5	0.14@300K	11.5-12.5	0.35@300K	11.5-12.5	0.2@300K
IR3(WV)	6.5-7.0	0.15@300K	6.5-7.0	0.09@300K	6.5-7.0	0.22@300K	6.5-7.0	0.12@300K
IR4(SWIR)	3.5-4.0	0.18@300K	3.8-4.0	(NA)			3.5-4.0	0.088@300K
Spatial resolution at nadir	VIS: 1km IR1-4: 4km		VIS: 1km IR1,2,4: 4km,IR3: 8km		VIS: 1.25km IR1-3: 5km		VIS: 1km IR1-4: 4km	
Num. of quantization levels	VIS: 1024 IR: 1024		VIS: 1024 IR: 1024		VIS: 64 IR: 256		VIS: 1024 IR: 1024	
Observing frequency (time/day)	Full disk: 24 Half disk:24(N.H.) 8 (S.H.)		Full disk: 24 (hourly) 4 (wind) Half disk: 13		Full disk: 24 (hourly) 4 (wind)		Full disk: 24 Half disk:24(N.H.) 8 (S.H.)	

2 Tracking of Sea Ice Motion

2.1 Maximal Cross Correlation Method

Figure 1 outlines the cross correlation method. The maximal cross correlation method uses two temporally successive images. In the earlier time image, select a rectangular-shaped reference of the object to trace, which is called a template.

From the later time image, select the search area with the same center as the template, where characteristics similar to those of the template are searched. Select a template of a set of pixels of the image as:

$$X = \{x_{(-t,-t)}, ..., x_{(t,t)}\} \tag{2.1}$$

where $x_{(i,j)}$ is a pixel value of the albedo and the center of the template is translated to (0,0). And select the same shaped set in the search area as:

$$Y_{(p,q)} = \{y_{(-t+p,-t+q)}, ..., y_{(t+p,t+q)}\} \tag{2.2}$$

where (p, q) is the center of $Y_{(p,q)}$. Then, the cross correlation coefficient is defined as follows:

$$Cor(X, Y_{(p,q)}) := \frac{\sum_{j=-t}^{t}\sum_{i=-t}^{t}(x_{(i,j)} - m(X))(y_{(p+i,q+j)} - m(Y_{(p,q)}))}{\sqrt{\sum_{j=-t}^{t}\sum_{i=-t}^{t}(x_{(i,j)} - m(X))^2}\sqrt{\sum_{j=-t}^{t}\sum_{i=-t}^{t}(y_{(p+i,q+j)} - m(Y_{(p,q)}))^2}} \tag{2.3}$$

where $m(X) := \frac{1}{(2t+1)^2}\sum_{i,j} x_{(i,j)}$,

$$m(Y_{(p,q)}) := \frac{1}{(2t+1)^2}\sum_{i,j} y_{(p+i,q+j)}$$

and $-(s-t-1) \leqq p, q \leqq s-t-1$.

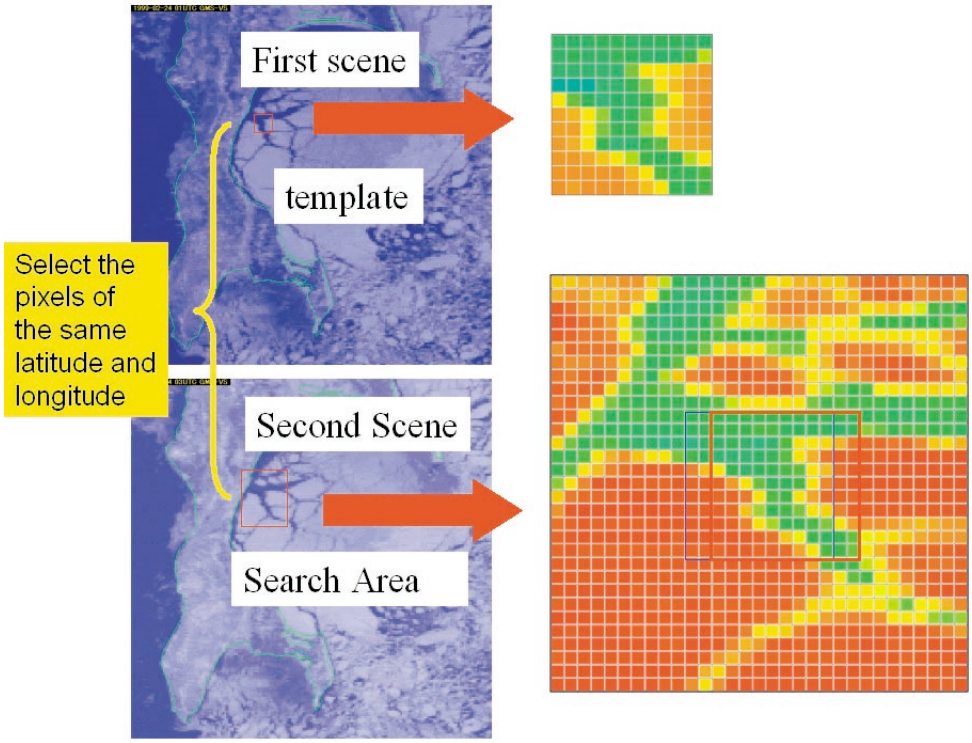

Figure 1. Brief overview of the cross correlation method. Select the reference set of pixels in the image taken at the earlier time and identify the set of pixels with the reference set of pixels by the cross correlation method. The blue rectangle represents the location of the template. The red rectangle represents the identified set of pixels in the search area.

For 11×11 the template and 31×31 the search area, t = 5, s = 15 and $-10 \leqq p, q \leqq 10$, here $(2s+1)^2$ is the size of the search area. The identified rectangular-shaped set of pixels is selected by the maximality of the cross correlation coefficient in the search area.

And, when (p', q') is the center of the identified rectangle, the velocity of sea ice motion is calculated as (p', q'). The displacement counted by the number of pixels is converted into the real velocity in terms of the location of the center of the template.

The value of the cross correlation coefficient (2.3) is invariant under the transformation $X \to aX + b$ and we can identify images that have uniformly different brightness temperatures in the entire region of the compared images (Johnson and Leone 1964, Matsumoto 2000). This is important when using visible images taken at long intervals because the reflection of sunlight depends on the solar zenith angle.

2.2 Size of template and search area

In Figure 1, the size of the template is selected as the width of 11×11 pixels. About half of the example template is made up of sea ice pixels and the other half is made up of lead pixels. Here, lead means the gap between the ice floes. Sea ice in the Sea of Okhotsk is generated and developed in the winter. As sea ice develops, the leads in the ice field are formed by the effects of wind and sea surface currents.

The leads and ice floes separated by the leads are recognized as the tracers of sea ice motion derivation by cross correlation coefficients.

The proportion of sea ice in the template is important for selecting the size of the template. When the size of lead is large, the number of pixels of sea ice decreases in the template. In this case the pixels of sea ice are recognized as noise. Therefore, it is necessary to select a size of template that is at least the width of 11×11 pixels, for recognizing a lead slightly larger than this size as the tracer of sea ice, too.

For example, consider the deformation of cross correlation coefficients as follows:

$$Cor(X,Y) = \frac{\sigma_X}{\sigma_Y} + \frac{1}{(2t+1)^2 \sigma_X \sigma_Y} \sum_{j=-t}^{t} \sum_{i=-t}^{t} R_{i,j}(X,Y). \quad (2.4)$$

Here,

$$R_{i,j}(X,Y) = (y_{(i,j)} - x_{(i,j)})(x_{(i,j)} - m(X)), \quad (2.5)$$

where X is the template and Y is the identified image.

σ_X and σ_Y are the standard deviations of the dataset X and Y, respectively. These equations are deformed from the result in the appendix to the notation of the pair of indices (i, j). $R_{i,j}$ indicates the contribution of a pixel to the cross correlation coefficient, and the distribution of it is shown in Figure 2. From Figure 2(c), it is clear that the sea ice area and lead area are distinguished remarkably, which suggests that the lead area makes a high contribution to the value of the cross correlation coefficient in this case. From this Figure, a template of this size is good to trace a sea ice lead of this size and the lead is recognized as a good tracer of sea ice. Every winter a lead of this size appears in this region. This region is located on the east side of Sakhalin. And, this size of lead is relatively large in the Sea of Okhotsk. If the size of the template is larger, the fine structure of sea ice cannot be detected. And, an adequate size for the template is near the width of 11×11 pixels.

The velocity of sea ice is about $0.6m/s$. The displacement of sea ice in two hours is calculated as about 5 pixels. Therefore, the size of the search area is selected as the width of 31×31 pixels (Kimura and Wakatsuchi 2001, Matsumoto 2000), in consideration of the velocity of over this value.

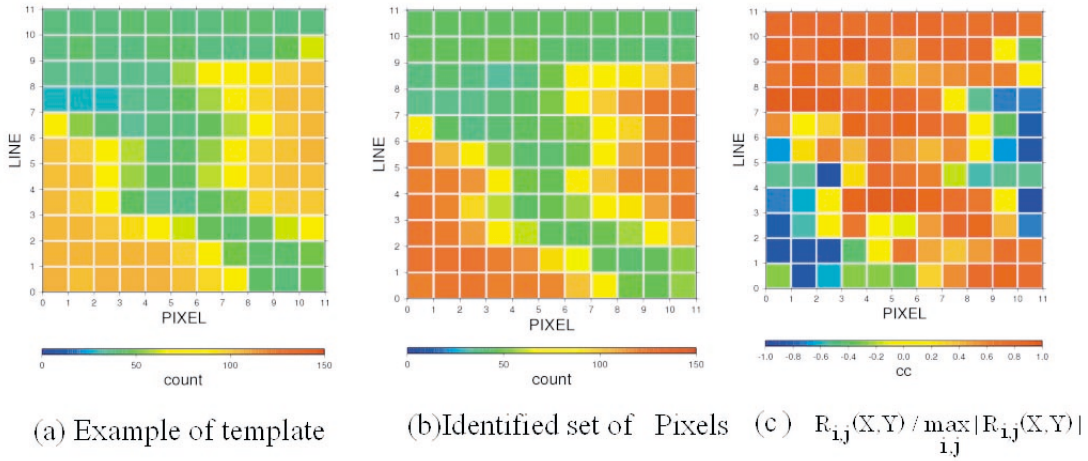

Figure 2. Example of template, identified set of pixels in search area and the value of Ri,j(X,Y).

2.3 Characteristics of derived vectors

Figure 3 shows the example of derived vector distribution. In the sea ice region (a), the derived vectors have a uniform direction. On the contrary, in the sea region (b), the derived vectors have random directions. By this difference of distribution of vectors, the area of sea ice can be separated from other areas. We introduce statistical values of entropy and uniformity in the directions to evaluate the difference. They are discussed in the next section.

If the final point cannot be detected in a relatively large area, the vector field in it should be a random vector field (Matsumoto, 2000, Ninnis et al., 1986). When the object moves beyond the search area, the maximal point of cross correlation coefficient is one of the spurious correlation peaks. These peaks are thought to be calculated by the fluctuations of satellite data.

3 Statistical values for extracting sea ice motion vector

To extract sea ice motion, two statistical values are introduced in this section.

To calculate statistical values evaluating the uniformity of vector distribution, a dataset of vector fields that is as dense as possible is needed.

The motion vector is calculated on every pixel in the image. Then the statistical values are calculated with the dataset of vectors contained in the finite area.

The width 9×9 of pixels is used in the definition of statistical values. The reason for setting the width of calculating area of statistical values is mentioned in the following section. We need to tune the size of the finite area by scale analysis of the sea ice physics, in future.

3.1 Entropy method

3.1.1 Definition of entropy

In usual image analysis, entropy is defined as the equation

$$S(X) = -\sum_i P(X_i) \log\{P(X_i)\}, \qquad (3.6)$$

where i denotes the index of brightness temperature and the $P(X_i)$ is the proportion of pixel number to brightness temperature index i in the event of brightness temperature $X = \{X_1, X_2, \ldots, X_n\}$. Here, X_i represents the event of the set of pixel value i in calculating area of entropy, and $0 \times \log(0) = 0$.

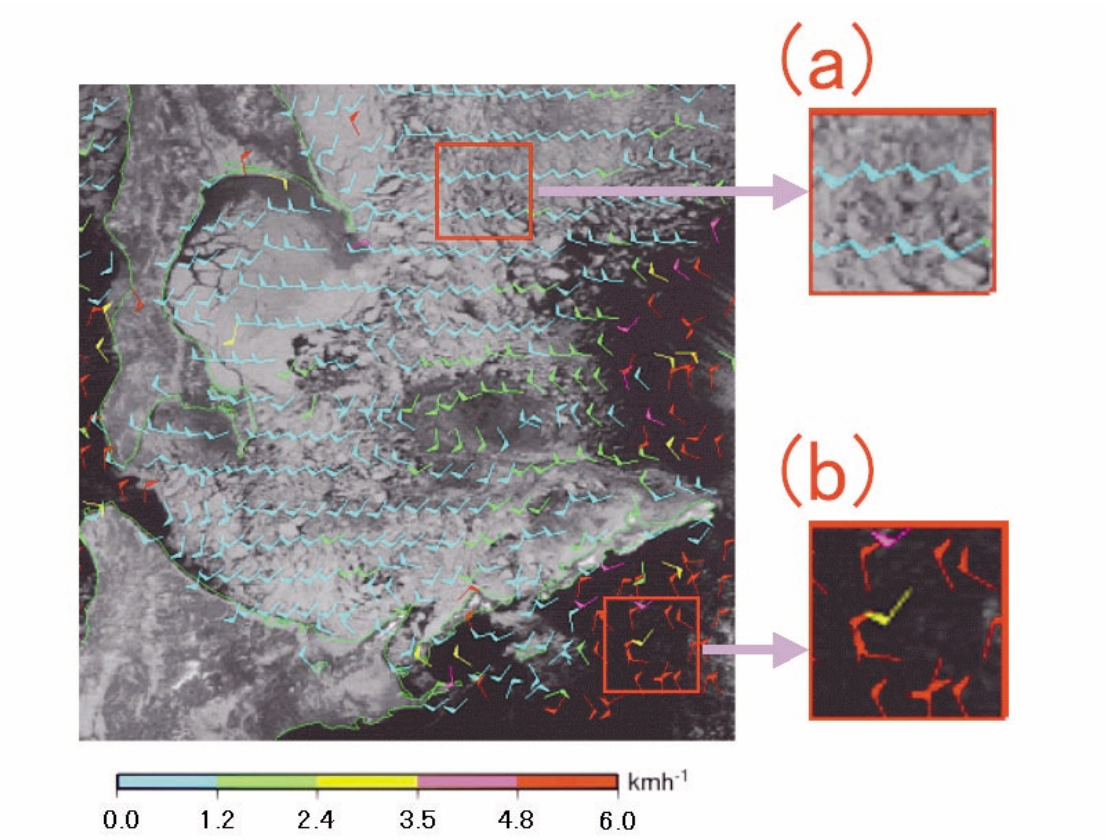

Figure 3. Example of motion vector field calculated from geostationary meteorological satellite 5 on February 24, 1999.

To define vector entropy, X is redefined as the calculating area of vector entropy as the set of sea ice motion vectors in a calculation width, and the center of X is transformed to $(0,0)$. I is defined as the set of the pair of indices of X, that is,

$$I = \{(i,j) : -4 \leq i,j \leq 4\}. \tag{3.7}$$

V is defined 9×9 as the set of all vectors in X, that is,

$$V = \{v_{(i,j)} : -4 \leq i,j \leq 4\}. \tag{3.8}$$

$I_{(p,q)}$ is defined as the set of the pair of indices, of which the velocity of east and west component is p, and that of north and south component is q, that is,

$$I_{(p,q)} = \{(i,j) \in I : v_{(i,j)} = (p,q), -15 \leq p,q \leq 15\}. \tag{3.9}$$

$\Delta(I_{(p,q)})$ is defined as the number of the elements in $I_{(p,q)}$.

Then, the proportion $P(I_{(p,q)})$ of $I_{(p,q)}$ in I is defined as follows:

$$P(I_{(p,q)}) = \frac{\Delta(I_{(p,q)})}{\Delta(I)}. \tag{3.10}$$

Using these definitions, the entropy of the distribution of vectors is defined in the same way as in the entropy of pixel values as follows:

$$S(V) = -\sum_{p,q} P(I_{(p,q)}) \log\{P(I_{(p,q)})\}. \tag{3.11}$$

If there are many same vectors in a finite area, entropy has a small value.

Examples of calculations are shown in following subsection.

However, it is not enough to use only entropy to

extract sea ice region because entropy doesn't take into account the quantity of vector uniformity.

For example, the following two cases (a) and (b) have the same entropy.

$$(a)\ P(I_{(1,1)}) = \frac{8}{9}, \quad P(I_{(1,2)}) = \frac{1}{9} \\ P(I_{(i,j)}) = 0, \quad (i \neq 1, \quad j \neq 1,2). \tag{3.12}$$

$$(b)\ P(I_{(1,1)}) = \frac{8}{9}, \quad P(I_{(1,4)}) = \frac{1}{9} \\ P(I_{(i,j)}) = 0, \quad (i \neq 1, \quad j \neq 1,4). \tag{3.13}$$

However (a) is more uniform than (b) obviously, because vector $(1,1)$ is more similar to vector $(1,2)$ than vector $(1,4)$. To evaluate the quantity of vector uniformity, the value of uniformity in a direction is introduced in next section.

3.1.2 Examples of calculation

First, calculate the ordinary entropy. Figure 4 shows the distribution of pixel values in 5×5 calculating the area. If the pixel values are all different from the other pixel values as in Figure 4(a), the value of entropy takes the highest values:

$$S(X) = -\sum_{i=1}^{25} \frac{1}{25} log(\frac{1}{25}) = log(25) \tag{3.14}$$

On the contrary, if each pixel takes the same value, the entropy is zero:

$$S(X) = -\sum_{i=1}^{25} 1 \times log(1) = 0. \tag{3.15}$$

For example, with the distribution of pixels as in Figure4 (b), the entropy is calculated as follows:

$$\begin{aligned} S(X) &= -\sum_{i=1}^{25} P_i log(P_i) \\ &= -\frac{7}{25} log(\frac{7}{25}) - \frac{6}{25} log(\frac{6}{25}) - \frac{4}{25} log(\frac{4}{25}) \\ &\quad - \frac{1}{25} log(\frac{1}{25}) - \frac{7}{25} log(\frac{7}{25}) \end{aligned} \tag{3.16}$$

$$= log(25) - \frac{1}{25}(14log(7) + 6log(6) + 4log(4)). \tag{3.17}$$

In almost the same way as calculating one-dimensional entropy, the entropy of vectors in Figure 5 is calculated as follows:

$$\begin{aligned} S(V) &= -\frac{7}{25} log(\frac{7}{25}) - \frac{10}{25} log(\frac{10}{25}) - \frac{5}{25} log(\frac{5}{25}) - \frac{3}{25} log(\frac{3}{25}) \\ &= log(25) - \frac{1}{25}(7log(7) + 10log(10) + 5log(5) + 3log(3)). \end{aligned} \tag{3.18}$$

1	16	19	20	24
2	18	23	22	21
14	15	25	17	12
6	7	13	10	9
3	4	5	11	8

(a) All pixels have different values.

1	1	2	20	20
2	2	1	2	2
14	15	1	20	20
14	1	14	14	1
1	2	20	20	20

(b) Pixels have above values.

Figure 4. Examples of entropy calculation of pixel values.

3.2 Value of uniformity in direction

3.2.1 Definition of uniformity in direction

As is shown in the appendix, first of all calculate the value of uniformity in direction for non-zero vectors (Matsumoto, 2003). Define the set of vectors in the calculating area as follows:

$$V_0 := \{v_{(i,j)} : v_{(i,j)} = (0,0)\}, \tag{3.19}$$

$$V_0{}^c := \{v_{(i,j)} : v_{(i,j)} \neq (0,0)\}. \tag{3.20}$$

And define the sets of indices corresponding to the sets V_0 and (Eq. (039)) as follows:

$$I_0 := \{(i,j) \in I : v_{(i,j)} \in V_0\}, \tag{3.21}$$

$$I_0{}^c := \{(i,j) \in I : v_{(i,j)} \in V_0{}^c\}. \tag{3.22}$$

Then,

$$D(V_0{}^c) := \frac{\left|\sum_{(i,j)\in I_0{}^c} v_{(i,j)}\right|}{\sum_{(i,j)\in I_0{}^c} \left|v_{(i,j)}\right|}. \tag{3.23}$$

$D(V_0{}^c)$ takes the maximum value of 1 when all vectors have an identical direction.

Here, the set of zero vectors does not contribute to this value, because $D(V)$ for the set of whole vectors $\bar{D}(V)$ is calculated as follows:

$$D(V) = \frac{\left|\sum_{(i,j)\in I_0{}^c} v_{(i,j)} + \sum_{(i,j)\in I_0} v_{(i,j)}\right|}{\sum_{(i,j)\in I_0{}^c} \left|v_{(i,j)}\right| + \sum_{(i,j)\in I_0} \left|v_{(i,j)}\right|} = \frac{\left|\sum_{(i,j)\in I_0{}^c} v_{(i,j)} + 0\right|}{\sum_{(i,j)\in I_0{}^c} \left|v_{(i,j)}\right| + 0}$$
$$= \frac{\left|\sum_{(i,j)\in I_0{}^c} v_{(i,j)}\right|}{\sum_{(i,j)\in I_0{}^c} \left|v_{(i,j)}\right|} = D(V_0{}^c). \tag{3.24}$$

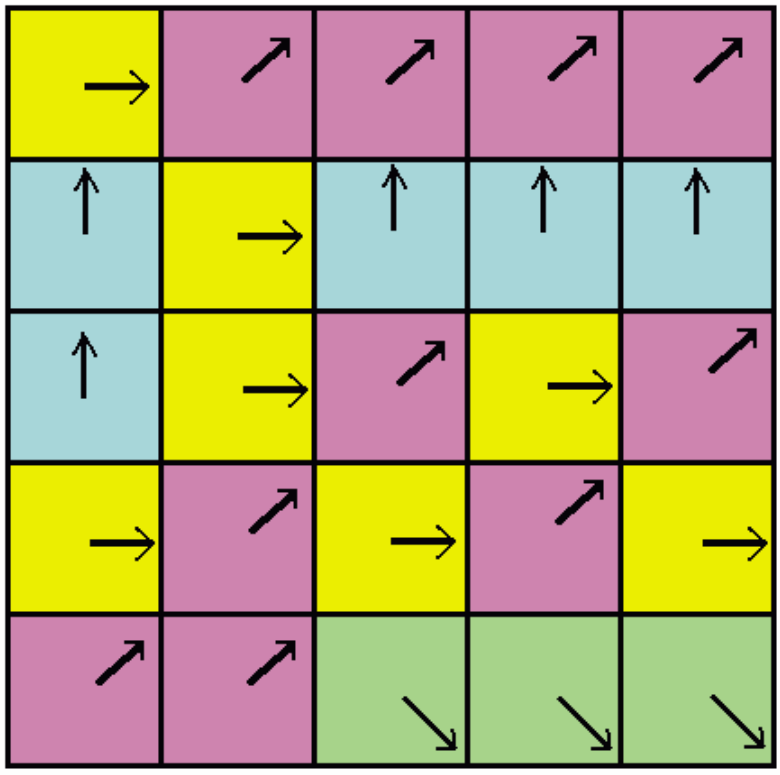

Figure 5. Distribution of vectors for calculating entropy.

Sea ice moves very slowly in contrast with wind. And in many cases sea ice is stationary, or has a subgrid scale displacement, because of the resolution of GMS. Therefore, it is a good way to consider the set of zero vectors derived from the cross correlation method as the vectors of uniform direction. To treat zero vectors that do not contribute to $D(V)$, the equation of the uniformity in direction $\bar{D}(V)$ is defined as follows:

$$\bar{D}(V) = (1 - P(I_0))D(V_0{}^c) + P(I_0) \times 1. \qquad (3.25)$$

3.2.2 Examples of calculation

For simplicity, the cases of three or four vectors are shown.

When the three vectors are balanced for each $\mathbf{v_i} \neq 0$ (Figure 6),

$$\mathbf{v_1} + \mathbf{v_2} + \mathbf{v_3} = 0. \qquad (3.26)$$

Therefore, $\bar{D}(\mathbf{V}) = 0$

When there are four vectors of balanced three vectors and another one vector (Figure 7),

$$\bar{D}(\mathbf{V}) = \frac{|\mathbf{v_4}|}{|\mathbf{v_1}| + |\mathbf{v_2}| + |\mathbf{v_3}| + |\mathbf{v_4}|}. \qquad (3.27)$$

When $\mathbf{v_i} = v_i \mathbf{v_0}$ for $i = 1, 2, 3, 4$,

$$\begin{aligned} \bar{D}(\mathbf{V}) &= \frac{|\mathbf{v_1} + \mathbf{v_2} + \mathbf{v_3} + \mathbf{v_4}|}{|\mathbf{v_1}| + |\mathbf{v_2}| + |\mathbf{v_3}| + |\mathbf{v_4}|} \\ &= \frac{|v_1\mathbf{v_0} + v_2\mathbf{v_0} + v_3\mathbf{v_0} + v_4\mathbf{v_0}|}{v_1|\mathbf{v_0}| + v_2|\mathbf{v_0}| + v_3|\mathbf{v_0}| + v_4|\mathbf{v_0}|} \\ &= \frac{|(v_1 + v_2 + v_3 + v_4)\mathbf{v_0}|}{(v_1 + v_2 + v_3 + v_4)|\mathbf{v_0}|} = 1. \end{aligned} \qquad (3.28)$$

According to the increase of the area of zero vectors, this value tends to 1. Therefore, this value would be the index of the proportion of the vectors with the same direction.

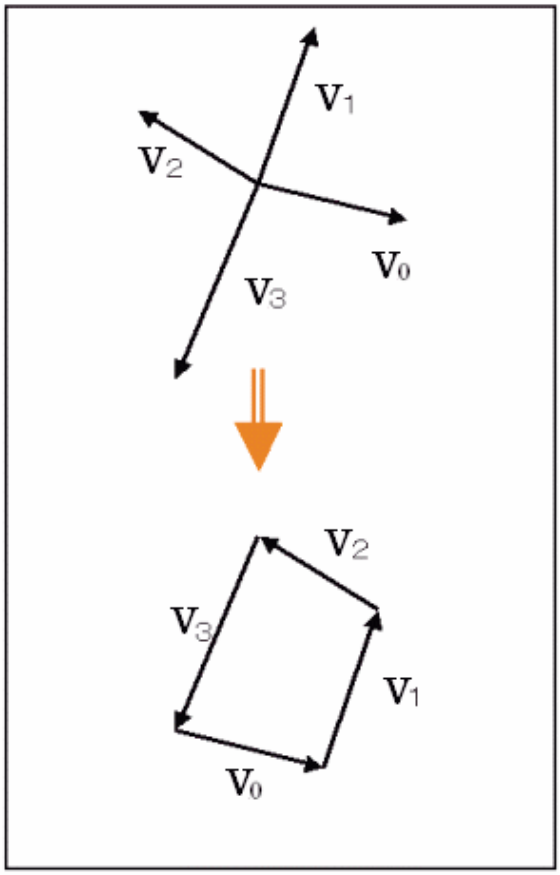

Figure 6. Example of set of vectors (1/2).

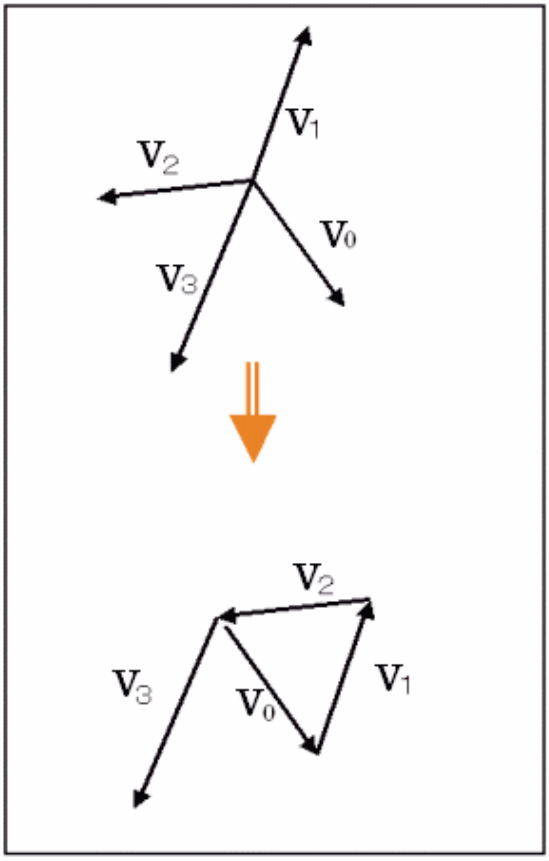

Figure 7. Example of set of vectors (2/2).

3.2.3 Another calculation

Set $\mathbf{u} = (u_1, u_2)$ and $\mathbf{v} = (v_1, v_2)$, where $u_i \geq 0$ and $v_i \geq 0$. Then

$$\mathbf{e_m}(\mathbf{u}, \mathbf{v}) = \frac{(u_1 + v_1, u_2 + v_2)}{\sqrt{(u_1 + v_1)^2 + (u_2 + v_2)^2}}. \quad (3.29)$$

Here,

$$\begin{aligned} |\mathbf{u}| \langle \mathbf{e_u}, \mathbf{e_m} \rangle &= \langle \mathbf{u}, \mathbf{e_m}(\mathbf{u}, \mathbf{v}) \rangle = \frac{u_1(u_1 + v_1) + u_2(u_2 + v_2)}{\sqrt{(u_1 + v_1)^2 + (u_2 + v_2)^2}}, \\ |\mathbf{v}| \langle \mathbf{e_v}, \mathbf{e_m} \rangle &= \langle \mathbf{v}, \mathbf{e_m}(\mathbf{u}, \mathbf{v}) \rangle = \frac{v_1(u_1 + v_1) + v_2(u_2 + v_2)}{\sqrt{(u_1 + v_1)^2 + (u_2 + v_2)^2}}, \\ \langle \mathbf{u}, \mathbf{e_m}(\mathbf{u}, \mathbf{v}) \rangle &+ \langle \mathbf{v}, \mathbf{e_m}(\mathbf{u}, \mathbf{v}) \rangle = |\mathbf{u} + \mathbf{v}|, \end{aligned} \quad (3.30)$$

where $\mathbf{e_m}$ is the unit vector in the mean vector direction. Here, $\mathbf{u} = |\mathbf{u}|\mathbf{e_u}$. Therefore,

$$\bar{D}(\mathbf{u}, \mathbf{v}) = \frac{|\mathbf{u} + \mathbf{v}|}{|\mathbf{u}| + |\mathbf{v}|}. \quad (3.31)$$

Here, $|\mathbf{u}| = \sqrt{{u_1}^2 + {u_2}^2}$. And the definition of uniformity in direction is satisfied.

If $\mathbf{u} = (1, 0)$ and $\mathbf{v} = (\cos\theta, \sin\theta)$, where $-\pi < \theta \leq \pi$, then $|\mathbf{u}| = 1$, $|\mathbf{v}| = 1$, $\mathbf{u} + \mathbf{v} = (1 + \cos\theta, \sin\theta)$, and $|\mathbf{u} + \mathbf{v}| = \sqrt{2(\cos\theta + 1)}$. Therefore,

$$\bar{D}(\mathbf{u}, \mathbf{v}) = \sqrt{\frac{1 + \cos\theta}{2}}. \quad (3.32)$$

4 Extracting sea ice motion vectors

Figure 8 shows a flow chart to extract sea ice motion vectors. First, prepare GMS visible data in the daytime. Sea ice is recognized using visible data. Second, use the cross correlation method to calculate sea ice motion vectors, as mentioned in the previous section. Third, use entropy and the value of uniformity in direction to extract sea ice traced vectors as a quality check. Two statistical values, entropy and the uniformity in direction are calculated in an area with a width of 9×9 pixels.

To select the size of calculating area of statistical values, the following five cases are possible: 5×5, 3×3, 7×7, 9×9 and 11×11, owing to the limit of setting the system. The case in which the width is 3×3 is not used because there is an insufficient quantity of information for the distribution of vectors.

The cases in which the width is 5×5 and 7×7, are not used, because there are a lot of pixels with

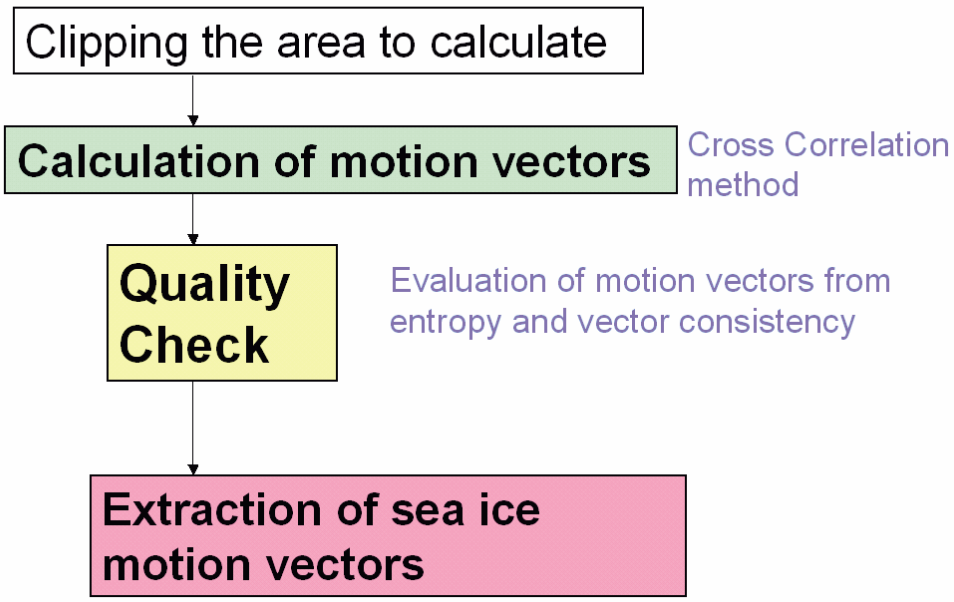

Figure 8. Vector extraction for flow of sea ice motion.

small entropy in the sea area, in contrast with Figure 9. Figure 9 is an example of the distribution of entropy, which is calculated when calculating areas with a width of 9×9. If areas with a width of 11×11 are used, the smallest scale for distinguishing sea ice is about $13.75 \times 13.75 km^2$, and phenomena on a smaller scale than this resolution cannot be recognized. Therefore, the size of the calculating area of entropy is set at a width of 9×9.

The width of the calculating area of the uniformity in direction is set to the same size as that of entropy, because the two values are comparable in terms of the distribution of statistical values.

Figure 9 shows the distribution of entropy and Figure 10 shows the value of uniformity in direction. Entropy gets larger according to the width of the calculating area because the vector field becomes more complicated as the size of the calculating area increases. First, the threshold of entropy is set at 0.4 for extracting the vectors on sea ice only. Next, set the threshold of entropy at 0.6 and that of the value of uniformity in direction at 0.8 for the following reasons: the threshold 0.6 of entropy is a slightly looser restriction to extract sea ice motion, and the threshold of uniformity in direction is selected as a value of 0.8 to add adequate sea ice motion vectors. And, these thresholds are set not to extract the vectors in the sea area. Figure 10 shows that the value of uniformity in direction has some ambiguities, in contrast with the entropy. This is why entropy is the main gauge for extracting sea ice motion.

The area (a) and (b) in Figure 3 can be distinguished by these statistical values. The derived vectors, thinned out at 0.25 degree intervals, are plotted in

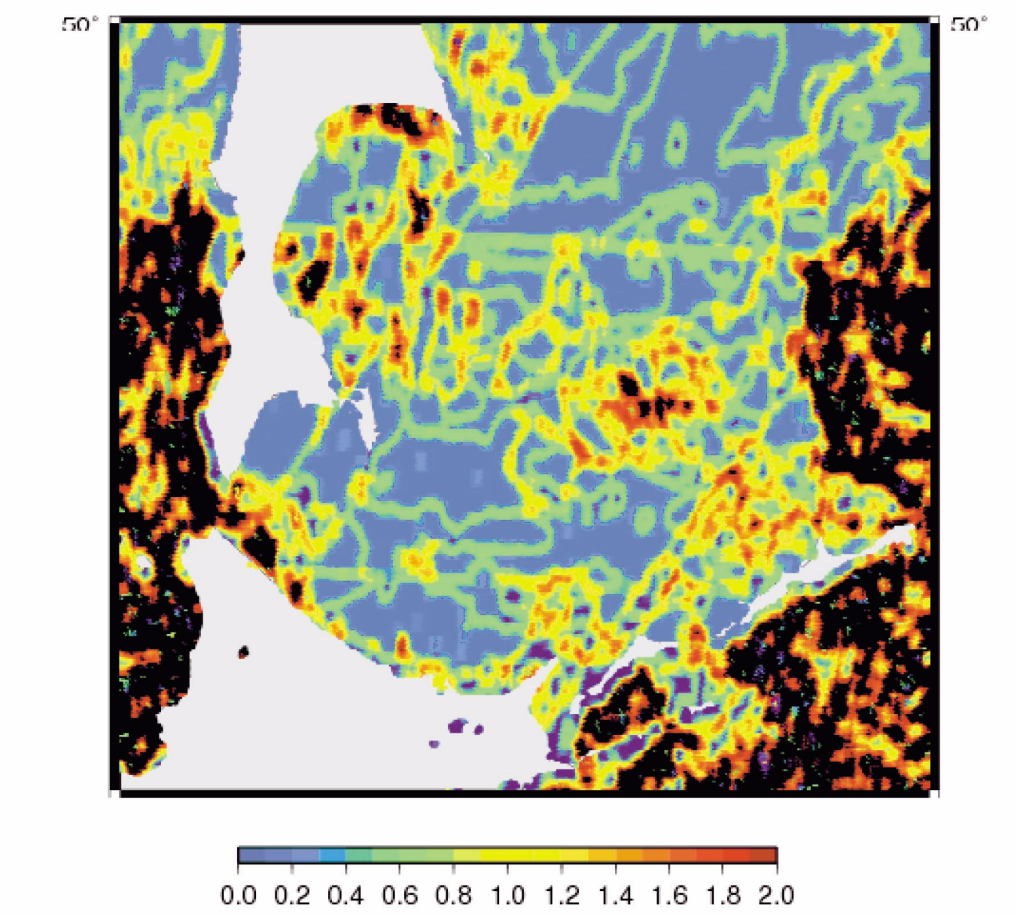

Figure 9. Distribution of entropy of Figure 2. The black area shows an entropy of more than 2.0.

Figure 3. (a) is the area where the vectors have an identical direction. On the other hand, (b) is the area where vectors do not have identical directions.

Setting the entropy threshold at 0.6 and the value of uniformity in direction threshold at 0.8, the sea ice traced vectors are extracted as in Figure 11.

Figure 12 shows the number of extracted vectors in cross correlation process (blue) and the number of survived vectors in the QC process (red). This figure shows the tendency of the calculated vectors in the whole area in the Sea of Okhotsk. The blue line in Figure 12 shows that the vectors are distributed in a displacement from 5.0 to 15.0 pixels.

On the other hand, the velocity of sea ice is about from 0 to 5 pixels per two hours (Kimura and Wakatsuchi 2001). Therefore, the threshold of the velocity to extract only sea ice motion cannot be determined in this method. The result in Figure 13 is comparable to the sea ice area analyzed in the sea ice analysis chart issued by JMA.

From Figures 11 and 12, the vectors are recognized to be distributed on the sea ice. Therefore, the derived motion vectors reflect the motion of sea ice.

5 Conclusion

Entropy and uniformity in direction are used in the quality check for the directive property of derived motion vectors. With a time scale of 2 hours, the sea ice motion vectors are calculated as the vectors of spatially ordered. Here, only these characteristics of sea ice motion vectors are treated. For this treatment, it is important to determine where a good reference is.

On the contrary, sea ice motion in eddies and the outflow of sea ice into the Pacific Ocean cannot be extracted. To extract sea ice motion vectors in eddies, it is necessary to investigate the other statistical values for extracting vectors, selection of the size of the template and the setting of thresholds, and so on.

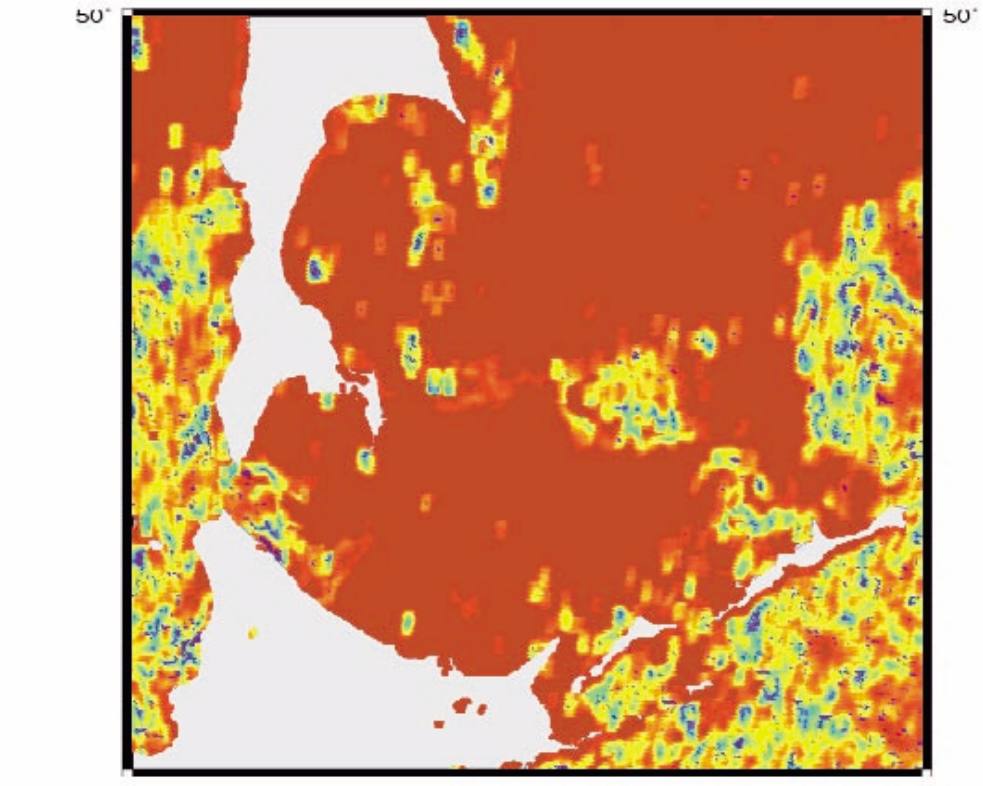

Figure 10. Distribution of uniformity in direction of Figure 2.

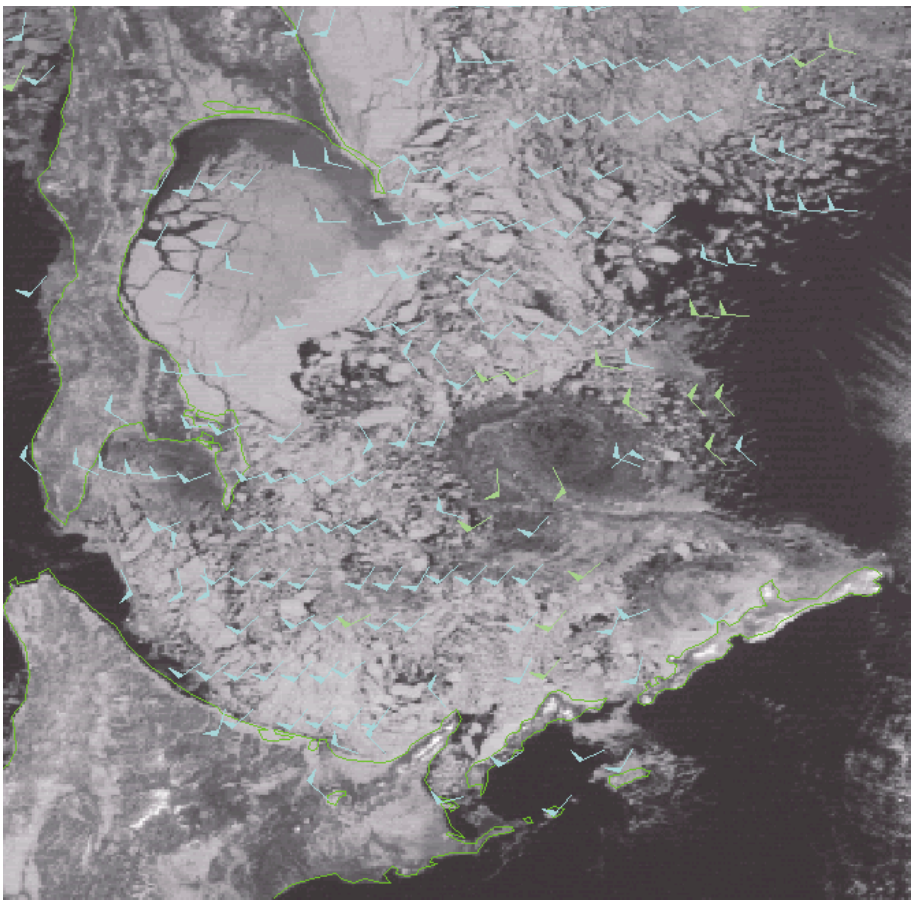

Figure 11. Extracted vector of sea ice motion from Figure 2.

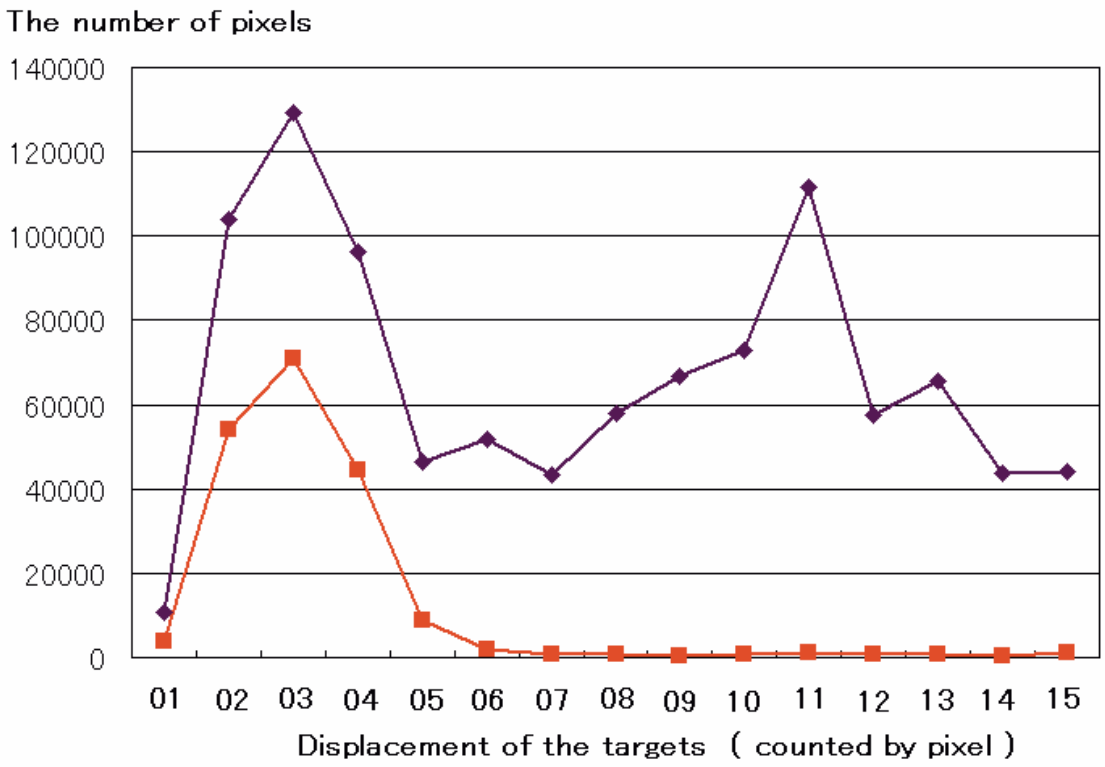

Figure 12. Distribution of the velocity of motion vectors. The blue line is the number of motion vectors. The red line is the number of processed vectors. Fractions of pixels are rounded up and objects with 0 displacement are included in the 01 level.

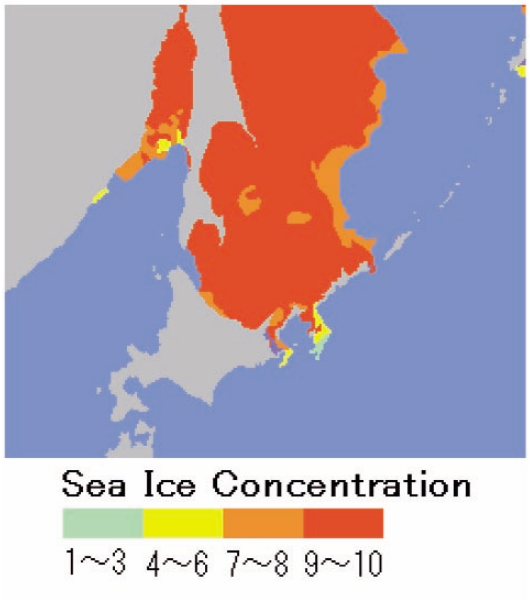

Figure 13. Sea ice analysis chart for February 25, 1999.

Acknowledgement

This paper was made from the presentation in the National Snow Ice Data Center (NSIDC), University of Colorado on March 16, 2007. Drs. Ted Scambos and Walt Meier advised Matsumoto about the sea ice characteristics and taught him how NSIDC derivates sea ice motion vectors. And many thanks to Director Roger G. Barry who encouraged one of the authors, Matsumoto, to write this paper. Drs. Bruce Raup, Ted Scambos, Walt Meier, and Director Roger G. Barry invited Matsumoto to NSIDC.

The Figures in this paper were made by Mr. Oyama and Mr. Miyakawa. And Mr. Myakawa checked the descriptions in this paper. From Dr. Noriaki Kimura suggestions about sea ice motion, the uniformity in direction was made by Matsumoto in 2003.

And, many thanks to the referees.

References

Emery, W. J., C. W. Fowler and J. A. Maslanik, 1995: Satellite Remote Sensing of Ice Motion, Oceanographic Applications of Remote Sensing, CRC Press, 367-379.

Johnson, N. L. and F. C. Leone, 1964: Statistics and Experimental Design in Engineering and Physical Science, Vol.1, Second edition, John Wiley and Sons, 454-457.

Kimura, N. and M. Wakatsuchi, 2001: Mechanisms for the variation of sea-ice extent in the Northern Hemisphere, J. Geophys. Res., 106(C12), 31319-31332.

Matsumoto, T., 2000: Extraction of Sea Ice Motion Vectors in the Sea of Okhotsk from Geostationary Meteorological Satellite Imagery, Journal of Meteorological Research Vol. 52, No. 2, 45-66.

Matsumoto, T., 2003: Sea Ice motion Vector in the Sea of Okhotsk by the Geostationary Meteorological Satellite Imagery, Journal of Meteorological Research Vol. 55, No. 1-2, 15-29.

Ninnis, R. M., W. Emery and M. J. Collins, 1986: Automated Extraction of Pack Ice Motion from Advanced Very High Resolution Radiometer Imagery, J. Geophys. Res. 91, 10725-10734.

Shannon, C. E. 1948: A Mathematical Theory of Communication, Bell System Technical Journal, vol. 27, pp 379-423, 623-656, July, October.

Appendix

A.1 Derivation of (2.4)

For simplicity, set the template of the image as the set of pixels $X = \{x_1, x_2, \ldots, x_n\}$ and the identified set of pixels as $Y = \{y_1, y_2, \ldots, y_n\}$ (Figure 14). Then, the equation of cross correlation coefficient is

$$Cor(X,Y) = \frac{\sum_{i=1}^{n}(x_i - m(X))(y_i - m(Y))}{\sqrt{\sum_{i=1}^{n}(x_i - m(X))^2}\sqrt{\sum_{i=1}^{n}(y_i - m(Y))^2}}$$

(Appendix 33),

where n is the dimension of the sequence of values of pixels and $m(X)=\frac{1}{n}\sum_{i=1}^{n}x_i$. Figure 3 shows the order of the sequence of the pixels.

The numerator of the cross correlation coefficient (Appendix 33) can be deformed as follows,

$$\begin{aligned}
&\sum_{i=1}^{n}(x_i-m(\mathbf{X}))(y_i-m(\mathbf{Y}))\\
&=\sum_{i=1}^{n}(x_i-m(\mathbf{X}))(y_i-x_i+x_i-m(\mathbf{X})+m(\mathbf{X})-m(\mathbf{Y}))\\
&=\sum_{i=1}^{n}(x_i-m(\mathbf{X}))^2+\sum_{i=1}^{n}(x_i-m(\mathbf{X}))(y_i-x_i)\\
&\qquad+\sum_{i=1}^{n}(x_i-m(\mathbf{X}))(m(\mathbf{X})-m(\mathbf{Y}))\\
&=\sum_{i=1}^{n}(x_i-m(\mathbf{X}))^2+\sum_{i=1}^{n}(x_i-m(\mathbf{X}))(y_i-x_i)\\
&\qquad+(m(\mathbf{X})-m(\mathbf{Y}))\sum_{i=1}^{n}(x_i-m(\mathbf{X}))\\
&=\sum_{i=1}^{n}(x_i-m(\mathbf{X}))^2+\sum_{i=1}^{n}(x_i-m(\mathbf{X}))(y_i-x_i)\\
&\qquad+(m(\mathbf{X})-m(\mathbf{Y}))\{\sum_{i=1}^{n}x_i-n\cdot m(\mathbf{X})\}\\
&=\sum_{i=1}^{n}(x_i-m(\mathbf{X}))^2+\sum_{i=1}^{n}(x_i-m(\mathbf{X}))(y_i-x_i)\\
&\qquad+(m(\mathbf{X})-m(\mathbf{Y}))\times 0\\
&=n\cdot{\sigma_X}^2+\sum_{i=1}^{n}(y_i-x_i)(x_i-m(\mathbf{X}))
\end{aligned}$$

(Appendix 34)

where $\sigma_{\mathbf{X}}^2=\frac{1}{n}\sum_{i=1}^{n}(x_i-m(\mathbf{X}))^2$.

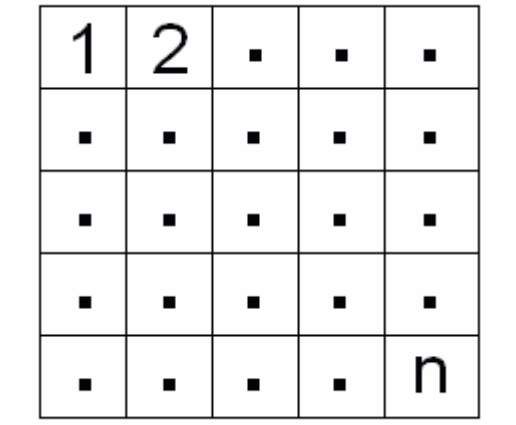

Figure 14. Order of sequence of pixels for simplification of cross correlation coefficient

Then

$$\begin{aligned}
Cor(\mathbf{X},\mathbf{Y}):&=\frac{\sum_{i=1}^{n}(x_i-m(\mathbf{X}))(y_i-m(\mathbf{Y}))}{\sqrt{\sum_{i=1}^{n}(x_i-m(\mathbf{X}))^2}\sqrt{\sum_{i=1}^{n}(y_i-m(\mathbf{Y}))^2}}\\
&=\frac{n{\sigma_X}^2+\sum_{i=1}^{n}(y_i-x_i)(x_i-m(\mathbf{X}))}{n\sigma_{\mathbf{X}}\sigma_{\mathbf{Y}}}\\
&=\frac{\sigma_{\mathbf{X}}}{\sigma_{\mathbf{Y}}}+\frac{1}{n\cdot\sigma_{\mathbf{X}}\sigma_{\mathbf{Y}}}\sum_{i=1}^{n}(y_i-x_i)(x_i-m(\mathbf{X}))\\
&=\frac{\sigma_{\mathbf{X}}}{\sigma_{\mathbf{Y}}}+\frac{1}{n\cdot\sigma_{\mathbf{X}}\sigma_{\mathbf{Y}}}\sum_{i=1}^{n}R_i(\mathbf{X},\mathbf{Y})
\end{aligned}$$

(Appendix 35).

A.2 Derivation of (3.23)

For the set of non-zero vectors $\mathbf{V}=\{\mathbf{v}_1,\mathbf{v}_2,\ldots,\mathbf{v}_n\}$,

$$\begin{aligned}
D(\mathbf{V}):&=\frac{|\sum_{i=1}^{n}\mathbf{v}_i|}{\sum_{j=1}^{n}|\mathbf{v}_j|}\\
&=\frac{|\sum_{i=1}^{n}\mathbf{v}_i|^2}{\sum_{j=1}^{n}|\mathbf{v}_j||\sum_{k=1}^{n}\mathbf{v}_k|}\\
&=\frac{\langle\sum_{i=1}^{n}\mathbf{v}_i,\sum_{i=l}^{n}\mathbf{v}_l\rangle}{\sum_{j=1}^{n}|\mathbf{v}_j||\sum_{k=1}^{n}\mathbf{v}_k|}.
\end{aligned}$$

(Appendix 36).

Using the averaged vector $\mathbf{m}(\mathbf{V}):=\frac{1}{n}\sum_{i=1}^{n}\mathbf{v}$,

$$\frac{\sum_{i=1}^{n}v_i\langle\mathbf{e_i},\mathbf{e_m}\rangle}{\sum_{i=1}^{n}|\mathbf{v_i}|}.$$

(Appendix 37)

Here, $\mathbf{e_m}$ is the unit vector of the direction of mean vector, and $\mathbf{v_i}=v_i\mathbf{e_i}$. When $m(\mathbf{V})=0$., the angle between $m(\mathbf{V})$ and each $\mathbf{v_i}$ cannot be defined. So in a while, suppose $m(\mathbf{V})\neq 0$.

$\frac{v_i}{\sum_{i=1}^{n}|\mathbf{v_i}|}$, (for i=1,...,n) are the proportion of the number of $\langle\mathbf{e_i},\mathbf{e_m}\rangle$ for the total vectors. The uniformity of direction $D(V)$ is defined as follows:

$$D(\mathbf{V})=\frac{\sum_{i=1}^{n}v_i<\mathbf{e_i},\mathbf{e_m}>}{\sum_{i=1}^{n}|\mathbf{v_i}|}.$$

(Appendix 38).

Here,

$$\sum_{i=1}^{n}\mathbf{v_i} = n|m(\mathbf{V})|\mathbf{e_m} = |\sum_{i=1}^{n}\mathbf{v_i}|\mathbf{e_m}. \quad \text{(Appendix 39).}$$

So,

$$\text{Numerator of D}(\mathbf{V}) = \sum_{i=1}^{n} v_i \langle \mathbf{e_i}, \mathbf{e_m} \rangle = \left\langle \sum_{i=1}^{n} v_i \mathbf{e_i}, \mathbf{e_m} \right\rangle$$
$$= n|m(\mathbf{V})| \langle \mathbf{e_m}, \mathbf{e_m} \rangle = |\sum_{i=1}^{n}\mathbf{v_i}|.$$

(Appendix 40).

And then,

$$D(\mathbf{V}) = \frac{|\sum_{i=1}^{n}\mathbf{v_i}|}{\sum_{i=1}^{n}|\mathbf{v_i}|}. \quad \text{(Appendix 41).}$$

This equation satisfies the case, $m(\mathbf{V}) = 0$ (Matsumoto, 2003). By using the angle θ_i^m between respective vectors $\mathbf{e}_i$ and averaged unit vector $\mathbf{e}_m := \frac{1}{|\sum_{i=1}^{n}\mathbf{v}_i|}\sum_{i=1}^{n}\mathbf{v}_i$, is calculated as follows:

$$< \mathbf{e_i}, \mathbf{e_m} >= |\mathbf{e_i}| \cdot |\mathbf{e_m}| cos(\theta_i^m) = cos(\theta_i^m).$$

(Appendix 42).

静止気象衛星データからの海氷移動ベクトルの抽出方法

松本　隆則[1]、今井　崇人[2]

要　旨

気象庁は、毎冬季、オホーツク海の海氷をモニターしている。海氷は風、海流及び潮汐により動かされる。時空間的に局所的な風、海流、潮汐の観測は少ない。それゆえに、衛星データから海氷の動きを計ることは有効である。

この論文では、静止気象衛星からの海氷移動ベクトルの算出とノイズの除去について述べる。2種類の統計量を定義し、閾値を設定することにより、海氷の移動のみが抽出でき、海氷以外の対象物からの影響は殆ど除去できた。

この論文は、Matsumoto 2000及び2003のレビューである。調査に利用されたスキームは、2007年1月から、衛星センターで利用されている。新しく定義した$R_{i,j}$はテンプレートの大きさを確定するのに利用されている。そして、海氷移動ベクトルの抽出方法の解説が本論文の目的である。

[1] 気象衛星センターデータ処理部システム管理課

[2] 気象衛星センターデータ処理部システム管理課（現所属：気象庁予報部予報課）